Acta Biomaterialia 65 (2018) 112–122

Contents lists available at ScienceDirect

Acta Biomaterialia

journal homepage: www.elsevier.com/locate/actabiomat

Full length article

Laponite nanoparticle-associated silated hydroxypropylmethyl cellulose as an injectable reinforced interpenetrating network hydrogel for cartilage tissue engineering

Cécile Boyer [a,b,1], Lara Figueiredo [a,b,1], Richard Pace [a,b], Julie Lesoeur [a,b,d], Thierry Rouillon [a,b], Catherine Le Visage [a,b], Jean-François Tassin [e], Pierre Weiss [a,b,c,*], Jerome Guicheux [a,b,c,2], Gildas Rethore [a,b,c,2]

[a] Inserm, UMR 1229, RMeS, Regenerative Medicine and Skeleton, Université de Nantes, ONIRIS, Nantes F-44042, France
[b] Université de Nantes, UFR Odontologie, Nantes F-44042, France
[c] CHU Nantes, PHU4 OTONN, Nantes F-44042, France
[d] SC3M, SFR Santé F. Bonamy, FED 4203, UMS Inserm 016, CNRS 3556, Nantes F-44042, France
[e] CNRS UMR6283, Institut des Molécules et Matériaux du Mans (IMMM), Université du Maine, Le Mans F-72000, France

ARTICLE INFO

Article history:
Received 17 August 2017
Received in revised form 20 October 2017
Accepted 7 November 2017
Available online 8 November 2017

Keywords:
Hydrogel
Cartilage
Biomaterial
Tissue Engineering

ABSTRACT

Articular cartilage is a connective tissue which does not spontaneously heal. To address this issue, biomaterial-assisted cell therapy has been researched with promising advances. The lack of strong mechanical properties is still a concern despite significant progress in three-dimensional scaffolds. This article's objective was to develop a composite hydrogel using a small amount of nano-reinforcement clay known as laponites. These laponites were capable of self-setting within the gel structure of the silated hydroxypropylmethyl cellulose (Si-HPMC) hydrogel. Laponites (XLG) were mixed with Si-HPMC to prepare composite hydrogels leading to the development of a hybrid interpenetrating network. This interpenetrating network increases the mechanical properties of the hydrogel. The *in vitro* investigations showed no side effects from the XLG regarding cytocompatibility or oxygen diffusion within the composite after cross-linking. The ability of the hybrid scaffold containing the composite hydrogel and chondrogenic cells to form a cartilaginous tissue *in vivo* was investigated during a 6-week implantation in subcutaneous pockets of nude mice. Histological analysis of the composite constructs revealed the formation of a cartilage-like tissue with an extracellular matrix containing glycosaminoglycans and collagens. Overall, this new hybrid construct demonstrates an interpenetrating network which enhances the hydrogel mechanical properties without interfering with its cytocompatibility, oxygen diffusion, or the ability of chondrogenic cells to self-organize in the cluster and produce extracellular matrix components. This composite hydrogel may be of relevance for the treatment of cartilage defects in a large animal model of articular cartilage defects.

Statement of Significance

Articular cartilage is a tissue that fails to heal spontaneously. To address this clinically relevant issue, biomaterial-assisted cell therapy is considered promising but often lacks adequate mechanical properties. Our objective was to develop a composite hydrogel using a small amount of nano reinforcement (laponite) capable of gelling within polysaccharide based self-crosslinking hydrogel. This new hybrid construct demonstrates an interpenetrating network (IPN) which enhances the hydrogel mechanical properties without interfering with its cytocompatibility, O_2 diffusion and the ability of chondrogenic cells to self-organize in cluster and produce extracellular matrix components. This composite hydrogel may be of relevance for the treatment of cartilage defects and will now be considered in a large animal model of articular cartilage defects.

1. Introduction

Articular cartilage (AC) is frequently damaged due to trauma or degenerative diseases. The incidence of joint diseases is constantly

* Corresponding author at: Inserm, UMR 1229, RMeS, Regenerative Medicine and Skeleton, Université de Nantes, ONIRIS, Nantes F-44042, France.
E-mail address: pierre.weiss@univ-nantes.fr (P. Weiss).
[1] Co-first authors.
[2] Co-last authors.

https://doi.org/10.1016/j.actbio.2017.11.027
1742-7061/

increasing due to a rising life expectancy of the general population leading to a global public health issue. The AC tissue is mainly composed of a unique cell type (chondrocyte) embedded within an abundant extracellular matrix (ECM). Cartilaginous ECM is composed of proteoglycans (mainly aggrecans) and collagens (mainly type II, IX and XI). Additionally, AC tissue is aneural and avascular. These characteristics prevent AC from having intrinsic regenerative properties after injuries leading to an inescapable degeneration of the tissue that culminates in osteoarthritis. Therefore, repairing lost or injured cartilage represents a challenge for both clinical and scientific perspectives [1,2].

Several strategies have been developed including tissue engineering which consists in the association of cells (e.g. adipose stromal cells (hASC) and human nasal chondrocytes (hNC)) with biomaterials [3]. Biomaterials, and more specifically hydrogels, have been widely studied over the past years [4]. In the last few years, the authors of this body of work have developed a self-setting hydrogel consisting of silanized hydroxypropylmethyl cellulose (Si-HPMC). This Si-HPMC hydrogel has already been demonstrated to be a convenient matrix for the three dimensional (3D) culture of hASC and hNC [5–7]. Hydrogels are of particular interest in biotechnology, tissue engineering, and drug delivery applications due to their hydrophilic character, porous structure, high water content and often biocompatible nature [8–10]. Despite their many advantages, the stiffness of hydrogels is often two orders of magnitude lower than cartilage's (100–1000 kPa) [11]. This lack of mechanical properties usually limits their application to space-filling scaffolds used for the delivery of bioactive molecules and cells [12,13].

Throughout the literature, several strategies have been developed to tune the mechanical properties of hydrogels, e.g. polymerization rate, polymer concentration as well as particles, carbon nanotubes or fibers embedding. To reach higher stiffness, these strategies usually require high polymer or particle concentrations. Among all these strategies, we decided to use reinforcements capable of crosslinking and forming an interpenetrated network (IPN) with Si-HPMC to increase the mechanical properties without interfering with the oxygen diffusion or cell viability.

Silicate nanoclays have shown great abilities of self-assembly with polymers and hydrogel formation. Indeed, in recent years, there has been much interest in using various clay nanoparticles to modify the properties of polymeric hydrogels and obtain organic/inorganic hybrid hydrogels with enhanced storage modulus [14]. In particular, the laponite clays (XLG), which are disk-like nanoparticles with a diameter of 25 nm and a thickness of about 1 nm, have been utilized in previous studies along with polymers such as poly(lactide)-poly(ethylene oxide)-poly(lactide) triblock copolymers [15], poly(N-isopropylacrylamide) [16], poly(N-vinyl-2-pyrrolidone-co-acrylic acid) [17], poly(ethylene oxide) [18,19], or sodium humate and polyacrylamide to form nanocomposite hydrogels with enhanced mechanical properties. The faces of XLG are negatively charged while their slices are positively charged. These properties allow them to form a hydrogel with controlled gelling properties [20,21] resembling a "house of cards" structure. Controlling the gelling properties has numerous advantages, such as *in situ* gelling which allows for the delivery of cells and bioactive molecules to the tissue defects in a minimally invasive manner.

Within this context, our objective was to use a minimal amount of XLG nano-reinforcements to form an IPN with Si-HPMC to increase the mechanical properties without modifying the interactions and behaviors of our hydrogel in biological environments (cell survival, proliferation, and diffusion).

In this study, we synthesized cellularized composite hydrogels and evaluated their physicochemical properties such as viscosity, gel point, storage modulus and oxygen diffusion. Then, we characterized their *in vitro* cytocompatibility. Based on these preliminary results, the ability of selected composite hydrogels to support the *in vivo* chondrogenic activity of chondrocytes in subcutaneous pockets of nude mice was ultimately assessed.

2. Materials and methods

2.1. Materials

Silanized hydroxypropylmethyl cellulose (Si-HPMC) and the acidic buffer solution (ABS) at pH 3.2 were prepared in our laboratories according to previously published protocols [22,23].

2.2. Hydrogel formulation

Si-HPMC hydrogels were prepared according to the already published protocol [22,23]. Si-HPMC polymer was dissolved in 0.2 M NaOH aqueous solution (30.9 mg ml^{-1}, pH 12.5); then two dialyses with molecular weight cut off at 6–8 kDa were performed in 0.09 M NaOH aqueous solution. The dialyses eliminate the non-grafted 3-glycidoxypropyltrimethoxysilane, used for siloxane grafting onto the HPMC. The hydrogel precursor solution was then obtained by mixing 1 vol of the above Si-HPMC basic solution contained in one luer-lock syringe, with 0.5 vol of ABS in another luer-lock syringe, by interconnection of both syringes; the final pH is 7.4. To prepare a nanocomposite hydrogel, we used two different protocols (Fig. 1A). In protocol A, we dispersed the desired amount of XLG into the ABS. Then we mixed 1 vol of 3 % wt Si-HPMC basic solution with 0.5 vol of ABS containing XLG. In protocol B, we dispersed the desired amount of XLG into distilled water. Then we mixed 1 vol of 4 % wt Si-HPMC basic solution with 0.5 vol of ABS and with 0.5 vol of XLG solution. The XLG amount inside each hydrogel is given as weight percentages of XLG concerning the mass of pure Si-HPMC hydrogel (without XLG). It varied between 0 and 5 % wt/v with protocol A and between 0 and 1% with protocol B. More than 1% of XLG yielded too quickly of a gelation time when using protocol B.

2.3. Rheology and mechanical properties

2.3.1. Gel point and storage modulus measurements

The gel points were measured on HAAKE RheoStress RS300 rheometer (Thermo Scientific) using cone geometry (1°/60 mm). Liquid hydrogel precursor solutions were injected on the plate immediately after mixing and the measurements started 1–2 min later.

Storage (G') modulus was monitored as a function of time under oscillation frequency sweep (from 1 to 22 Hz) at constant temperature (23 °C). The gel point was determined when tan $\delta = G''/G'$ became independent from frequency. Each sample was measured in triplicate.

2.3.2. Dynamic mechanical analysis (DMA)

A volume of 2 mL of the Si-HPMC/ XLG liquid mixtures was injected into each well of 12-well plastic plates for cell culture which served as molds. We prepared hydrogel specimens of each XLG concentration (n = 3). To ensure the complete gelification, the samples were kept enclosed under a humid atmosphere at room temperature for 2 weeks. The 2-week old hydrogels were taken out of molds, and their diameters and heights were measured with a caliper. The DMA study in uniaxial unconfined mode was performed using BOSE ElectroForce® 3100 Test Instrument equipped with the WinTest® digital control system. The sinusoidal oscillations started at 5% deformation of the sample's height, and the oscillation amplitude reached 10% of the height. We then

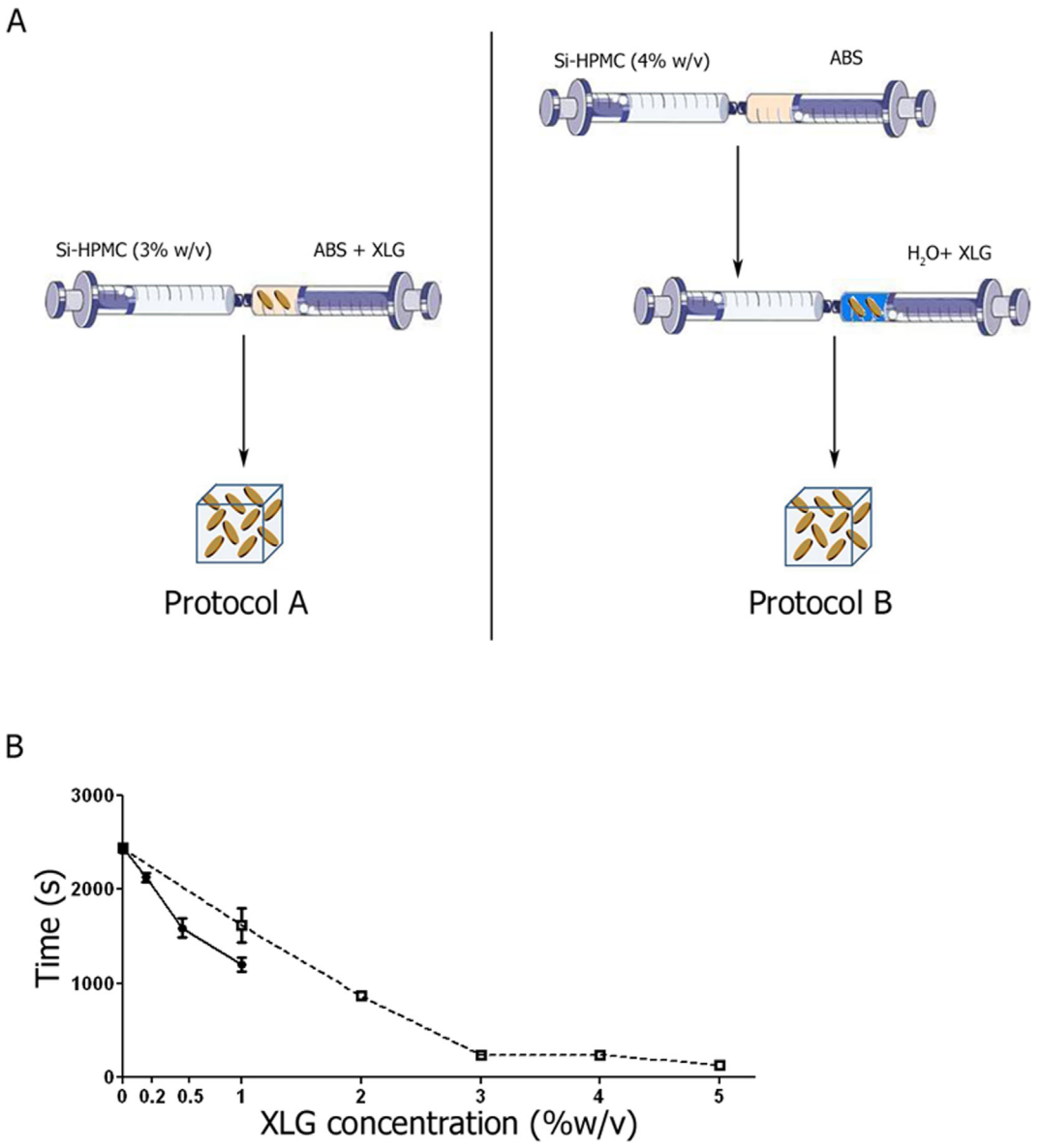

Fig. 1. Preparation protocols and rheological characterization (gel point) of Si-HPMC hydrogels as a function of of XLG concentration. (A) Schematic overview of Protocols A and B (ABS: acidic buffer solution). (B) Gel point of Si-HPMC hydrogels mixed with increasing concentrations of XLG was measured with a RS300 rheometer. Constructs were prepared with either protocol A (dashed line) or protocol B (solid line), as described in materials and methods section.

determined the real part E′ of the complex compressive modulus for each nanocomposite hydrogel at a frequency of 1 Hz.

2.4. Oxygen tension measurements

2.4.1. Oxygen measurements

Core oxygen (O_2) partial pressures in the 3D constructs were monitored with a needle type O_2 microsensor (PreSens, Germany). The optic fiber coated on a 140 μm flat-broken tip with sensitive PSt1 microsensor material (PreSens, Germany) is protected within a standard hollow needle. The sensor allows real-time O_2 measurements, without O_2 consumption, through dynamic fluorescence quenching, with data reported to an oxy-4 transmitter (PreSens, Germany). Since O_2 diffusion is a temperature dependent phenomenon, all measurements were performed at 37 °C.

For determination of O_2 content kinetics in acellular hydrogels (protocol B, Fig. 1A), samples prepared at atmospheric conditions were moved into a SCI-live Hypoxia Workstation (Ruskinn, Pencoed, UK), at 37 °C and 5% CO_2 with O_2 levels set at 0.1%. Deoxygenation of the hydrogel samples (with the tip of the O_2 microsensors positioned in the center of the construct) was followed until equilibrium was reached, after which re-oxygenation was monitored in a 5% CO_2, 37 °C humidified incubator in normoxic conditions (20%).

2.5. Scanning electron microscopy (SEM)

For the SEM experiments, samples of Si-HMPC hydrogel containing laponites were embedded in an acrylic resin obtained by polymerization of a mixture of Glycol Methacrylate (GMA) and n-Butyl Methacrylate (BMA) monomers. Samples were gently dehydrated by soaking them in gradually concentrated baths of GMA monomer with water until to finish by several baths in 100% of GMA. They were then impregnated overnight at 4 °C in a mixture of (GMA/BMA) monomers with catalyst peroxide compound before to be transferred in gelatin capsules and to be cured

during several days from 37 °C to 60 °C. After polymerization, blocks of samples embedded in resin were lapped and polished using a grinder-polisher (MetaServ2000, BUEHLER) and then coated with a thin layer of amorphous carbon using a vacuum evaporator (JEE-4B, JEOL) before SEM observations. The SEM observations of embedded samples were performed using a scanning electron microscope (LEO 1450VP, ZEISS) operating at 9 kV or 15 kV and pictures were recorded from the back-scattered electron detector (BSE). A sample of Si-HMPC hydrogel containing laponites was also observed by SEM in its hydrated state using a WETSEM® sealed capsule having SiN windows (QX-102, QuantomixTM). SEM observations of the wet sample were performed at 20 kV, and pictures were recorded from the BSE mode.

2.6. Cell viability

2.6.1. Adipose stromal cell culture

To determine the viability of cells when cultured in the presence of our hydrogels, human adipose stromal cells (hASC) were used. ASC were obtained from human patients undergoing liposuction and who had given written consent (Agence de BioMedecine n ° PFS08-018, legislation code L.1211-3 to L.1211-9). hASC were isolated by collagenase digestion of lipoaspirates. Briefly, and as previously described [24], lipoaspirates were washed extensively with HBSS to remove debris, treated with collagenase and centrifuged at 250*g* for 5 min. hASC were cultured in a 5% CO_2 incubator at 37 °C in Dulbecco's modified Eagle's medium (DMEM) with Glutamax (Life Technologies, France) supplemented with 10% fetal bovine serum (FBS) and 1% penicillin/streptomycin.

2.6.2. Cell viability in 2D

hASC viability was evaluated by methyl tetrazolium salt (MTS) assay (Promega, USA). Two different experiments were performed, (1) evaluation of hASC viability cultured in direct contact with increasing concentrations of XLG and (2) evaluation of hASC cell viability cultured in contact with Si-HPMC hydrogel containing increasing concentrations of XLG (protocol B, Fig. 1A). hASC were seeded onto culture plates and were allowed to attach to 48-well plates at a final density of 10,000 cells per cm^2. After 24 h, the culture medium was removed, and either XLG or Si-HPMC containing XLG was added onto the cell layer. For the culture in direct contact, 200 μL of culture medium containing 0.001, 0.01, 0.1 or 1% XLG (% w/v) were added to each well and refreshed every two days. For the culture in contact with hydrogel, 250 μL of Si-HPMC hydrogel containing 0%, 0.2%, 0.5% or 1% XLG were added per well. After 1 h of gelation at 37 °C, 200 μL of culture medium was added to each well and refreshed every two days. As a positive control for both experiments, hASC were cultured in the presence of actinomycin-D (5 μg/mL), a well-known inducer of cell death. Finally, MTS assay was performed at day 0, 1, 2, 3 and 6. The MTS assay is based on the reduction of MTS tetrazolium compound by viable cells that generates a colored formazan product soluble in the culture medium. The colored product was measured by the optical density reading at 490 nm (Victor^{3}V 1420 Multilabel Counter). Each condition was tested in quadruplicate.

2.6.3. Cell viability in 3D

3D cell viability was evaluated by Live/Dead Cell Viability assay (ThermoFisher Scientific, MA, USA) with hASC mixed into hydrogels (protocol B, Fig. 1A) at a final density of $1x10^6$ cells per mL of Si-HPMC. Si-HPMC hydrogels containing 0%, 0.2%, 0.5% or 1% XLG were molded and allowed to gelate in wells of a 48-well plate at 37 °C for 1 h. After gelation, 200 μL of culture medium were added to each well and refreshed every two days. As a positive control, hASC were cultured in 3D into Si-HPMC hydrogel in the presence of actinomycin-D (5 μg/mL). At day 0, 2 and 6, a Live/Dead Cell Viability assay was performed according to the manufacturer's instructions. A green fluorescence can be observed due to the calcein AM indicating the intracellular esterase activity. And a red fluorescence can be observed due to the ethidium homodimer-1 indicating the loss of plasmic membrane integrity. Living cells were stained green and dead cells were stained red. Red and green fluorescence were observed with a confocal microscope (Nikon D-eclipse C1 (Ar/Kr)). Each condition was tested in quadruplicate.

2.7. In vivo experiment

We embarked on *in vivo* experiments based on the subcutaneous implantation of well-known chondrogenic cells, namely human nasal chondrocytes (hNC), in conjunction with Si-HPMC/1% XLG hydrogel to investigate whether our hybrid biomaterial was able to support chondrogenesis (protocol B, Fig. 1A). The hNC were obtained from human patients undergoing rhinoplasty and who had given written consent (Agence de BioMedecine n° PFS08-018, legislation code L.1211-3 to L.1211-9). The hNC were isolated by enzymatic digestion of nasal cartilage as described previously [25]. Briefly, nasal cartilage was cut into small slices and digested at 37 °C with 0.05% hyaluronidase in HBSS for 10 min, then with 0.2% trypsin for 15 min and finally with 0.2% type II collagenase for 30 min. Finally, slices were digested overnight at 37 °C in 0.03% collagenase in DMEM. The suspended hNC were cultured in DMEM with Glutamax supplemented with 10% FCS, 1% penicillin/streptomycin. hNC were expanded at 37 °C in a humidified atmosphere of 5% CO_2 and culture medium was changed every 2–3 days.

Seven-week-old swiss nude female mice were used for the *in vivo* study (Charles River Laboratory, France). All animals were treated in accordance with the Medical Animal Care Guidelines of the University of Nantes (APAFIS#3082-201512081180278l6v 2). Si-HPMC hydrogels both with and without 1% XLG were mixed with hNC at 1, 2 and 5 × 10^6 cells/mL as described previously [25]. 250 μL of each cellularized hydrogel were injected subcutaneously in the back along each side of nude mice. The implantations were performed under general anesthesia using isoflurane gas (Halothane, Baxter, Switzerland) and under aseptic conditions. After six weeks, mice were euthanized, and hydrogels were individually explanted. Each explant was fixed in formaldehyde solution for subsequent histological analyses.

2.8. Histological analyses

All explants were fixed in 4% paraformaldehyde solution and embedded in paraffin. Embedded samples were sectioned (5 μm thick). After that paraffin sections were de-paraffinized using toluene, rehydrated through a graded series of ethanol and rinsed in distilled water. Tissue sections were stained with hematoxylin-eosin-safran (HES), alcian blue (AB) and Masson's Trichrome (MT) as described elsewhere [25,26]. Sections were finally visualized using a light microscope (Zeiss Axioplan 2, Göttingen, Germany).

2.9. Image analyses

After histological staining, slides were scanned, and images were analyzed by ImageJ software. Three squares (250 μm × 250 μm) were randomly defined on each image. Nodules of hNC were counted and their areas measured.

2.10. Statistical analysis

Results are expressed as mean ± SEM of triplicate determinations. Comparative studies of means were performed by using

Kruskal-Wallis test followed by a post hoc test (Dunn's Multiple Comparison Test) with statistical significance at $p < 0.05$.

3. Results

3.1. Rheology, mechanical properties, and microscope analysis

Our objective was to use nanoparticles to reinforce our hydrogel made of Si-HPMC polymer. First, the rheology investigation showed that the gel point, the time needed to reach the sol-gel transition of our hydrogels, decreases when the concentration of XLG increases (Fig. 1B). Moreover, the protocol (A or B) used for the formulation of the composite hydrogels seems to not influence the gel point, reaching in both cases 1500 s at 1% wt/v of laponites.

As depicted in Fig. 2, adding XLG within Si-HPMC induces an increase in the mechanical properties when compared to Si-HPMC hydrogel alone. The storage moduli of the Si-HPMC/XLG hybrid constructs were tested using shear stress and DMA compression experiments (G' and E' respectively). Regardless of the technique used, the results obtained showed the same behavior with an increase in the storage moduli when the quantity of added XLG increases. The E' modulus of Si-HPMC hydrogel is approximately 5 kPa. Upon increasing the XLG amount, an increase of E' was observed. The increase of XLG amount in hydrogel allowed the modulus to reach a 4-fold increase for 5% XLG mixed with protocol A and a 3-fold increase for only 1% of XLG mixed with protocol B. It is worth noting that it was not possible to prepare XLG loaded at a concentration higher than 1% with protocol B. The gel point was reached almost instantly when using more than 1% XLG making the mixing process impossible.

Following the mechanical investigations, microscopic observations were performed to deeply investigate the structural differences of the composite hydrogels depending on the protocol used. When XLG are dispersed in ABS before mixing with Si-HPMC, XLG remained in aggregates (Fig. 3A, D), while when XLG are dispersed in water before mixing with Si-HPMC, they formed

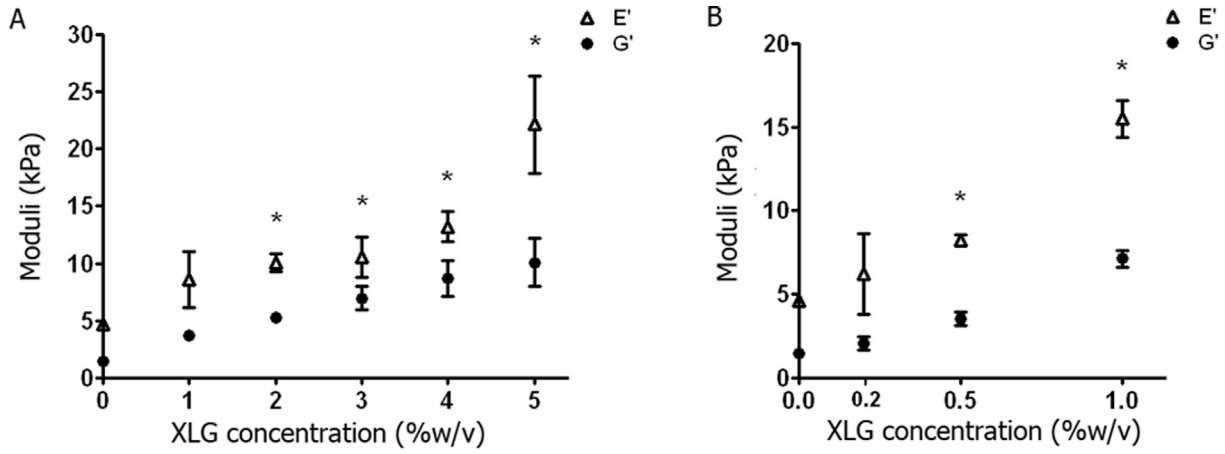

Fig. 2. Viscoelastic moduli G′ and E′ of Si-HPMC hydrogels containing increasing concentrations of XLG. The G′ modulus (dot) was measured with MARS rheometer while the E' modulus (triangle) was measured with DMA. Si-HPMC hydrogels mixed with increasing concentrations of XLG as indicated were tested. Hybrid constructs were prepared following 2 different protocols, protocol A (A) or B (B) as described in materials and methods. *$p < 0.05$ compared to the 0% XLG condition.

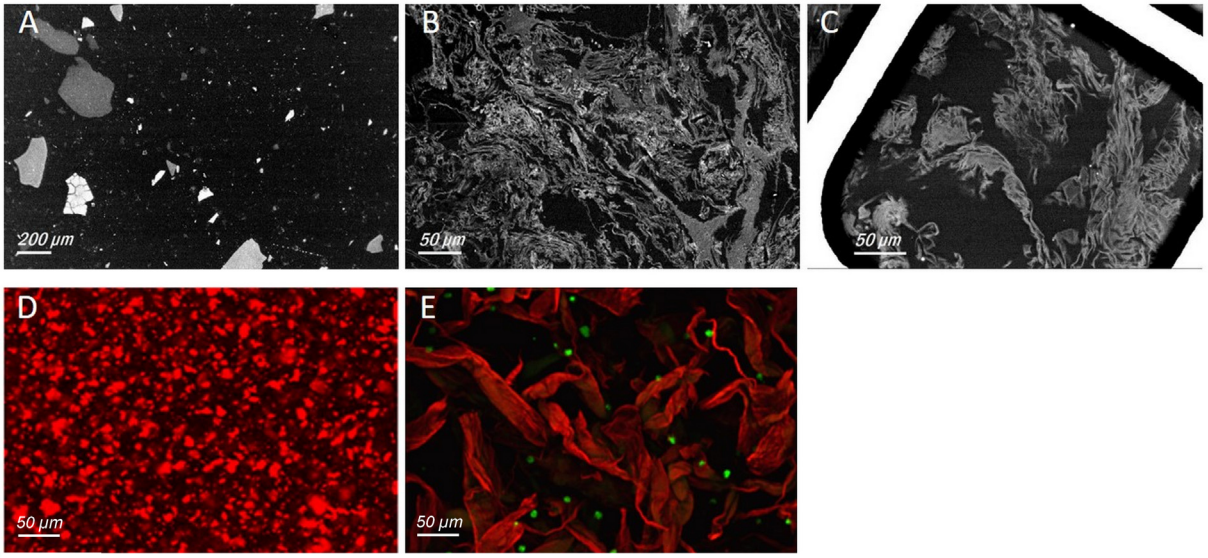

Fig. 3. Composite hydrogel ultrastructure. Microscopic analysis of Si-HPMC/XLG hydrogel prepared with protocol A. electronic (A: SEM) images showing the Si-HPMC/laponites structure and Confocal (D) image of Si-HPMC/XLG hydrogel stained in red. Microscopic analysis of Si-HPMC/XLG hydrogel prepared with protocol B: electronic (B: SEM, C: SEM in hydrated state using a WETSEM® sealed capsule) images showing the Si-HPMC/XLG structure and Confocal (E) image of hASC cells seeded within Si-HPMC/XLG hydrogel after Live&Dead® labelling: living cells were labelled with Calcein AM (green) and XLG with Ethidium homodimer-1 (red).

their network interpenetrated with Si-HPMC network (Fig. 3B, C, E). The dual network was observed under a confocal microscope with the formation of wave shape structures. Moreover, the use of WETSEM® sealed cap, allowed us to observe under SEM our composite hydrogel in its hydrated form, confirming the formation of an interpenetrating network.

3.2. Cellular viability in 2D and 3D

Our objective was then to evaluate the cytocompatibility of our scaffolds (i) in a 2D culture where the hydrogel is placed above the cell layer, and (ii) in a 3D culture where cells are cultured into our hydrogels.

XLG was found to alter MTS activity from 0.001% when hASC were cultured in direct contact with the XLG (Fig. 4A). However, regardless of XLG concentration, we failed to detect any alteration of MTS activity when cells were cultured in 3D within Si-HPMC/XLG (Fig. 4B).

To confirm these data, a double staining kit was then used for simultaneous staining of living and dead cells in 3D culture. Living cells are stained in green by calcein AM and dead cells in red by ethidium homodimer-1. Confocal analysis was performed on day 0, 2 and 6. Fig. 5 shows the 3D reconstructions of hybrid hydrogels associated with hASC. Cells cultured in 3D in the presence of actinomycin-D were used as a control of cell death. Confocal observations of Si-HPMC/XLG constructs showed the presence of green, living cells when hASC were cultured in 3D in this hybrid construct. The interpenetrated network can concomitantly be observed as XLG and ethidium homodimer-1 link together (due to electrostatic interactions) resulting in a red color of the XLG wave structures within the hydrogel.

3.3. Oxygen tension

Since XLG nanoparticles have been described as oxygen barrier [27,28], the O_2 diffusion was evaluated within Si-HPMC hydrogel

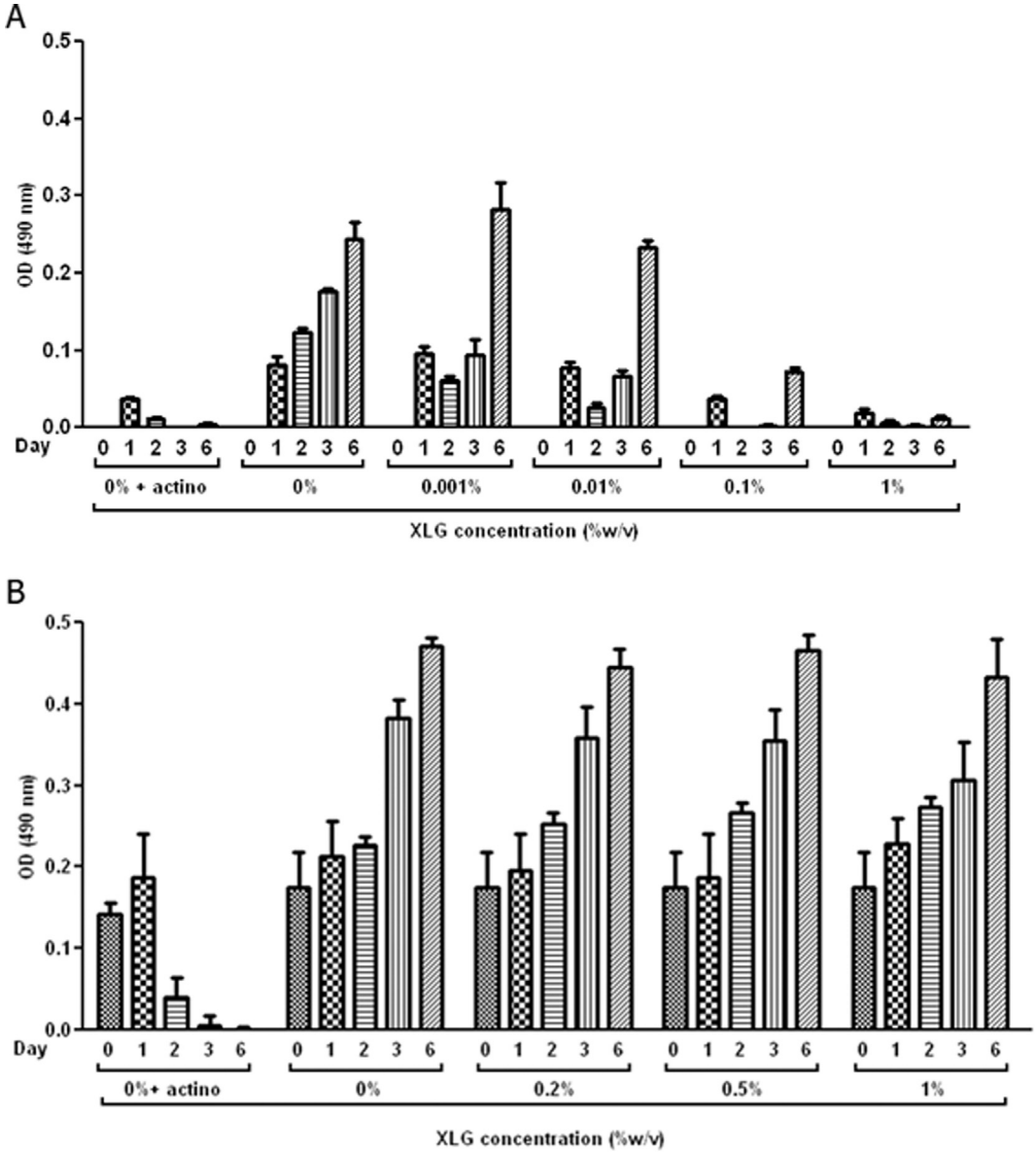

Fig. 4. MTS activity of hASC cultured in 2D. (A) hASC viability was evaluated in 2D after adding 0–1% XLG as indicated on top of the cell layer (10,000 cells/cm^2). (B) hASC viability was evaluated in 2D after molding Si-HPMC hydrogels with 0 to 1% XLG as indicated on top of the cell layer (10,000 cells/cm^2). As described in materials and methods, a MTS assay was performed at day 0, 1, 2, 3 and 6. Negative control (actino) was obtained by growing hASC in the presence of actinomycin D (5 μg/mL).

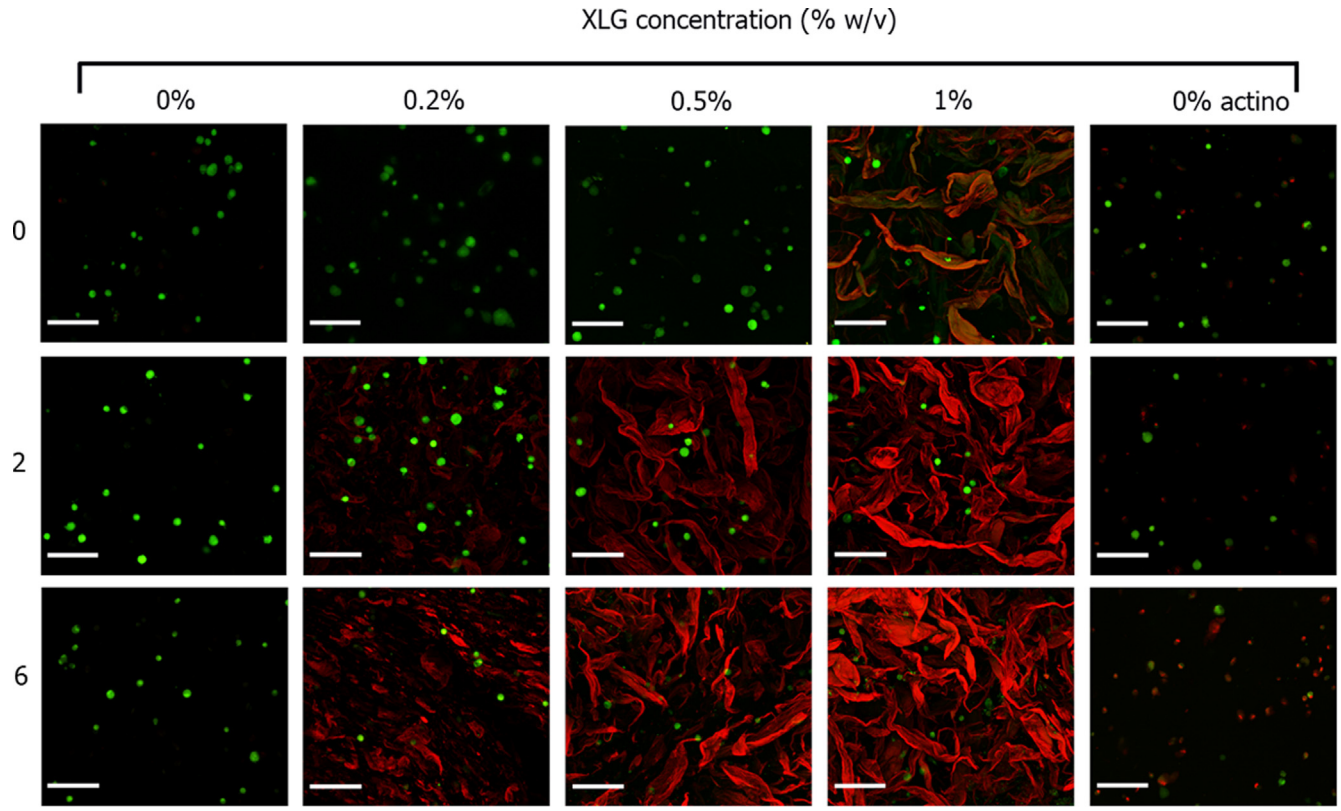

Fig. 5. 3D viability of hASC cultured into Si-HPMC hydrogel containing increasing concentrations of XLG. Human ASC viability was evaluated in 3D after molding Si-HPMC hydrogels containing increasing concentrations of XLG (0–1%) and mixed with 1 x 10^6 hASC at day 0 (0), 2 (2) and 6 (6) by Live/Dead Cell Viability assay. Living cells were stained by Calcein AM in green and dead cells were stained in red by ethidium homodimer-1. Negative control was obtained by adding actinomycin D (5 μg/mL) in the culture medium. XLG nanoparticules were also stained in red due to the electrostatic interaction with ethidium homodimer-1. Scale bar: 100 μm.

containing 1% XLG. O_2 diffusion has been monitored with and without XLG. No significant differences are observed between Si-HPMC and Si-HPMC/1% XLG constructs, both of which reached O_2 levels of around 17% at equilibrium. Acellular Si-HMPC hydrogels were prepared in atmospheric conditions and were then transferred to a controlled anoxic environment (0.1% O_2). Their de-oxygenation profile, represented as the first part of the curve in Fig. 6, shows no obvious differences between Si-HPMC and Si-HPMC/1%XLG constructs, with a slow decrease in their O_2 content. For both hydrogels, equilibrium (i.e. O_2 content of 0.1%) was reached after 60 h of incubation in anoxic conditions. The second part of the curve represents the re-oxygenation profile of hydrogels when they were transferred back to a normoxic environment (O_2 content of 20%). From this point, re-oxygenation profiles for both groups are once again superimposed, suggesting that 1% XLG addition to Si-HMPC hydrogel has no obvious effect on O_2 diffusion *per se*.

3.4. In vivo experiments

To determine whether 1% XLG-enriched Si-HPMC hydrogel may support *in vivo* chondrogenesis, we finally studied the subcutaneous implantation of robust chondrogenic cells (hNC) in combination with our biomaterial in a method described previously [7,25]. After harvest, isolation, and culture, hNC (1 to 5 × 10^6 cells/mL) were mixed with Si-HPMC or Si-HPMC/1% XLG hydrogels and injected in nude mice subcutis for 6 weeks.

As expected, samples containing Si-HPMC or Si-HPMC/1% XLG without hNC show neither cells nor coloration in the graft. Fig. 7 shows that hNC associated with Si-HPMC and Si-HPMC/1%XLG hydrogels are organized in nodules revealed in HES, AB and MT stainings. HES staining also indicated the presence of mature chondrocytes within lacunae surrounded by a basophilic matrix. Cells in the nodules secreted GAGs revealed in blue with AB staining, and collagens evidenced in green with MT staining. When 1% XLG was added to Si-HPMC, a lower amount of hNC nodules was observed into the explants. However, cells retain their ability to

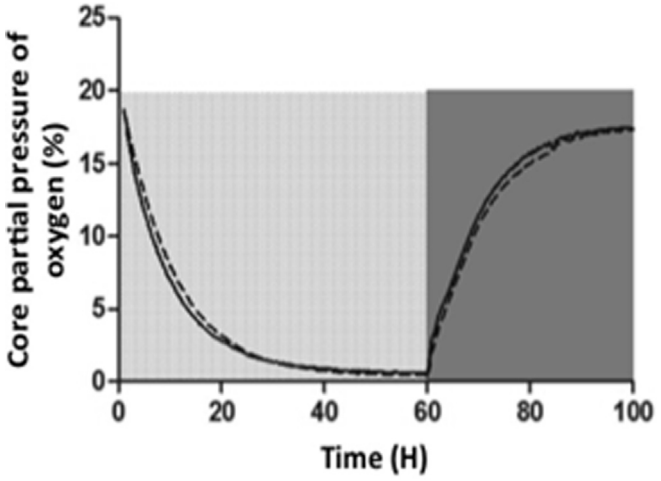

Fig. 6. Oxygen diffusion. De-oxygenation and re-oxygenation profiles of acellular Si-HPMC hydrogels (with (dashed line) or without (filled line) XLG) prepared in atmospheric conditions then transferred to hypoxic conditions (▒, 0.1% O_2) until equilibrium was reached, then transferred to normoxic conditions for re-oxygenation (■, 20% O_2). Results are presented as core partial pressure values measured in the center of the construct (mean value ± SEM, n = 4).

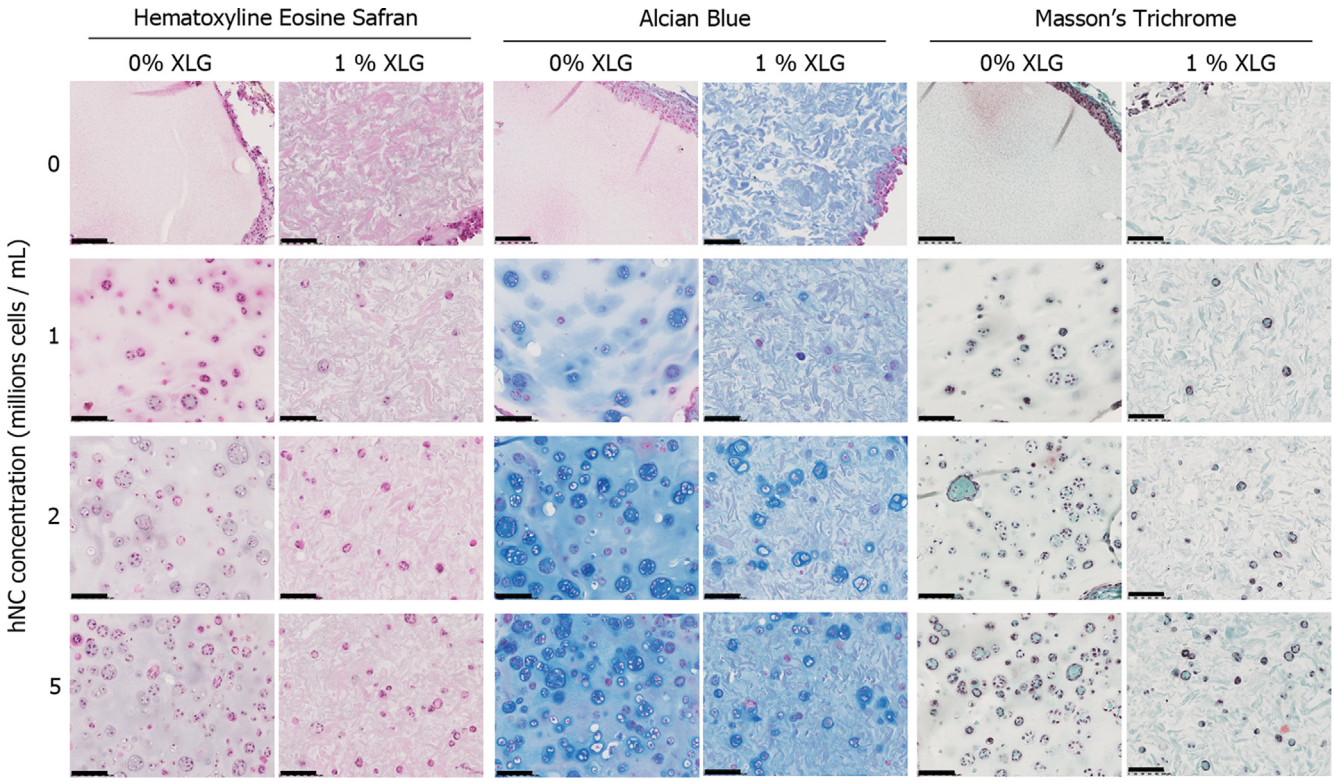

Fig. 7. Histological analysis of cartilaginous tissue formation after subcutaneous implantation of hNC with Si-HPMC/XLG hydrogels. 250 μL of Si-HPMC (0% XLG) or Si-HPMC/1% XLG (1% XLG) hydrogels mixed with hNC (cell density varying from 0 to 5 millions cells/mL of Si-HPMC) were implanted in subcutaneous pocket in nude mice. Both hydrogels without hNC were used as negative control (0). After 6 weeks, explanted samples were histologically prepared for Hematoxyline Eosine Safran, Alcian Blue and Masson's Trichrome staning. Scale bar: 100 μm.

self-organize in nodule and secret extracellular matrix components. It is worth noting that the number of nodules increases when more hNC are added during the mixing process. These results indicate that Si-HPMC/1% XLG support the formation of a cartilaginous tissue in nude mice subcutis when implanted with hNC.

Despite a significant reduction in a number of nodules and total area (Fig. 8A and B), nodules analysis shows that the area per nodule was not significantly affected by the presence of XLG.

4. Discussion

After injuries, articular cartilage shows limited repair properties leading to a progressive degeneration of the tissue that dramatically exposes the onset of osteoarthritis. Therefore, developing new regenerative therapy appears essential. Toward that goal, tissue engineering strategies, associating cells and biomaterials, have been developed. The development of biomaterials for mini-invasive surgery requires the matching of several parameters from physico-chemistry (e.g. rheology, self-hardening) to biology (e.g. cytocompatibility, biocompatibility, and biofunctionality). The physicochemical characterizations first consisted of determining the potential use of our hydrogel (Si-HPMC/XLG) in terms of handling such as the need to be injectable. The viscosity showed that there was no difficulty in injecting the solution and the gel point represents the working time during which the clinician can manipulate, mix the different components and inject the solution before it hardens. Then, mechanical investigations were performed to determine whether the composite hydrogels can withstand the mechanical stress of the implantation site. Fig. 2 showed that regardless of the protocol, the viscoelasticity of the hydrogel increases with the XLG concentration. The protocol with XLG first suspended in pure water showed a stronger reinforcement of the hydrogel reaching up to 15 kPa with 1% wt/v of XLG. This increase could help the biomaterial to last longer under the mechanical stress in the implanted site compared to Si-HPMC alone. The relative stability of the hydrogel is of particular relevance in tissue engineering strategies notably in articular cartilage regenerative medicine because it allows cells to produce a functional extracellular matrix conferring some mechanical properties comparable to that of native/healthy tissue to the newly formed tissue. This property is important for tissue engineering strategies to allow time for the encapsulated cells to secrete extracellular matrix for tissue renewal.

When particles are used to reinforce hydrogels, a large amount has to be added in order to get an increase of the modulus, such as 50% for calcium phosphate [29]. Lower amount of particles can be used in some cases such as silicate nanofibers where an increase of the storage modulus is obtained with only 5% of incorporation [30]. This property relies on the ability of the particle to covalently link to the polymer network. Moreover, Formica et al. showed that their PCL (polycaprolactone) fiber reinforced alginate scaffolds were able to stand longer subcutaneously and to produce large amount of cartilage specific ECM (extra cellular matrix) compared to their alginate scaffold alone [31–33].

Microscopic observations of the hydrogel prepared according to both mixing protocols showed drastic differences in the architectural structures. When XLG were suspended in the acid buffer, the composite hydrogels were composed of XLG aggregates within the Si-HPMC hydrogel. On the other hand, when XLG were in suspension in pure water, they formed wave-shaped structures leading to an interpenetrating network. Additionally, to further characterize the microenvironment for cell embedding, O_2 tension measurements have shown no significant influence of XLG on O_2

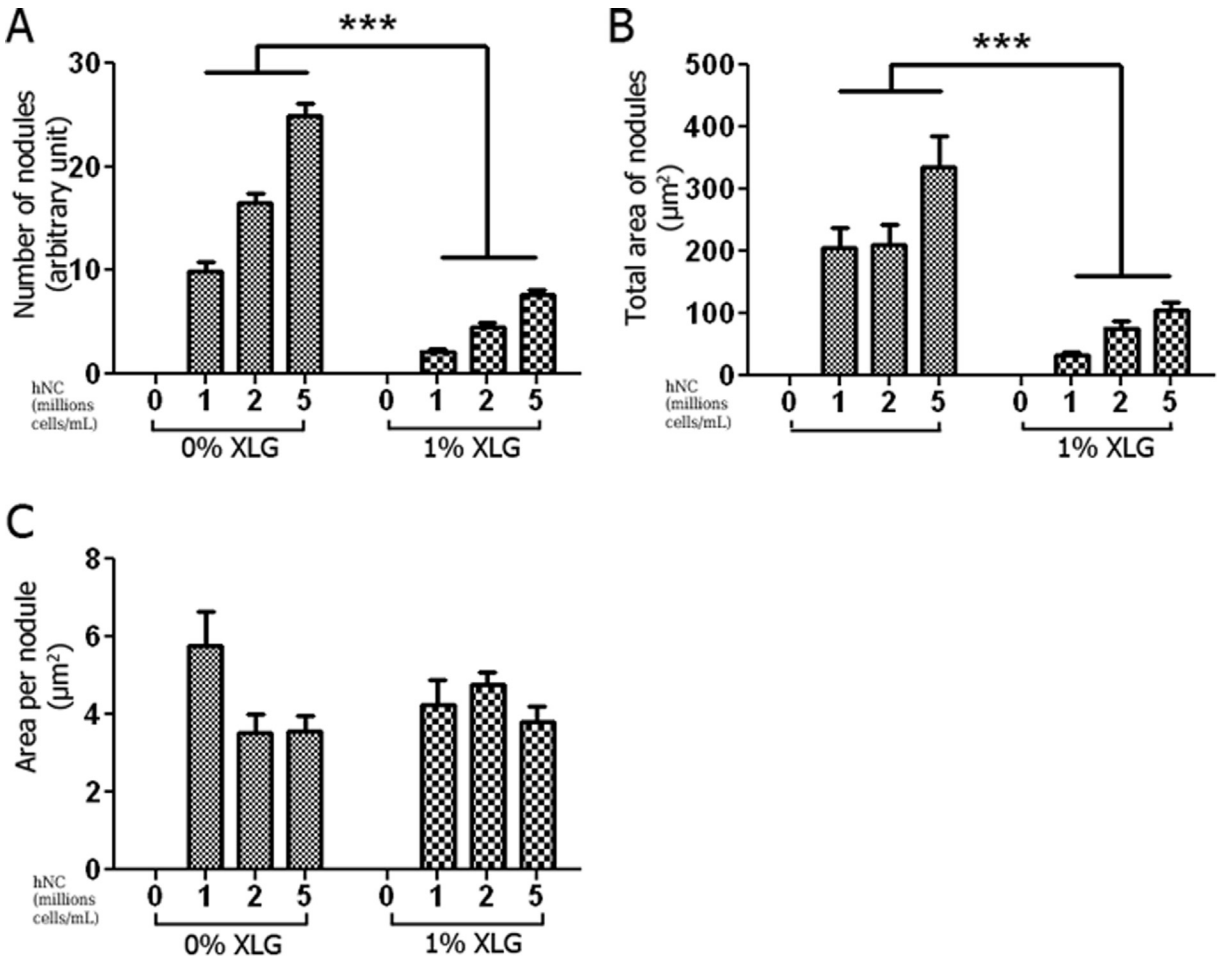

Fig. 8. Nodules analysis after histological staining. 250 µL of Si-HPMC (0% XLG) or Si-HPMC/1% XLG (1% XLG) hydrogels mixed with hNC (cell density varying from 0 to 5 millions cells/mL of Si-HPMC) were implanted in subcutaneous pocket in nude mice. After 6 weeks, explanted samples were histologically prepared for Hematoxyline Eosine Safran, Alcian Blue and Masson's Trichrome staning. Number of hNC nodules (A), total area of hNC nodules (B) and area per hNC nodule (C) have been determined by image analysis with ImageJ software. $^{*}p < 0.001$ compared to the 0% XLG condition.

tension and diffusion without cells. Put together, the ability of XLG to self-assemble and form double network leads to the increase in the mechanical properties of the final constructs without interfering with O_2 diffusion.

Based on the ability of XLG to form a double interpenetrating network, thereby increasing the mechanical properties, the XLG composite hydrogel was further investigated. MTS assay showed no modification of the mitochondrial activity up to 1% wt/v (10 mg/mL) of XLG in 2D. Live&Dead staining was then performed to confirm this result in 3D cell growth. Throughout the literature, the cytotoxicity of XLG has been studied for two main formulations (e.g. XLG suspensions and hydrogels). Indeed, Janer et al. investigated the toxicity of pristine and functionalized nanoclays [34]. They have demonstrated that the toxicity is mainly increased because of the presence of organic groups at the surface of XLG. However, XLG have been shown to be non-toxic only up to 10 µg/L (10^{-6}% wt/v). From 10 µg/L and onwards, the toxicity increased according to the concentration. In the meantime, few groups have been working on the development of silicate hydrogels. Ebato et al. have developed a nanocomposite hydrogel for 2D cell culture and they showed no toxicity of their structure [35]. Moreover, Orefo et al. prepared nanoclay-gel for cell encapsulation. They demonstrated the feasibility of their strategy, showing a very good viability in 3D and the ability to host the chondrogenic differentiation of human bone marrow stromal cells. In our strategy, XLG formed a gel and were mixed with Si-HPMC hydrogel. Altogether, these data suggest that cells can be grown within our composite hydrogel.

The ideal biomaterial for cartilage tissue engineering should not only allow for the maintenance of the chondrocyte differentiation but should also enable their transplantation via a mini-invasive surgical protocol *in vivo*. Consequently, to decipher whether Si-HPMC/XLG hydrogels could represent this ideal scaffold, we investigated its ability to support the transplantation of chondrogenic cells and the formation of cartilage tissue *in vivo*. To address this issue, we focused our attention on the use of cells exhibiting a reliable and robust chondrogenic potential such as hNC [36]. Interestingly, after six weeks *in vivo*, hNC were positively stained after respectively Alcian Blue and Masson Trichrome histology staining confirming that the entrapped hNC could still produce an extracellular matrix containing GAG and collagen. Also, a decrease in the number of clusters is shown when XLG is added to the construct. However, when the entrapped cell number increases, histology staining demonstrated that the number of the cluster also increased in the meantime. More importantly, the mean area per cluster remains unchanged independently of the initial amount of cells and the presence of XLG.

Consequently, the decrease in cells and cluster number could be due to an initial toxicity during the mixing process (1200 s before gel points (Fig. 1)) inducing cell death at the early time. Indeed, investigations on cells incubated with XLG suspension have shown 2D toxicity from 10 µg/L and onwards with drastic XLG internal-

ization inside the cells (data not shown). Before the gel point, XLG are free to move and could make contact with cells leading to their incorporation in the cytosol. After gel point, surviving cells may be able to multiply and form clusters. Regardless of the presence of XLG, the same behavior is observed such as an increase in the number of clusters when the concentration of the entrapped cells increases. To mitigate the initial cell death, the cell concentration has to be increased when XLG are mixed with Si-HPMC hydrogel. No significant difference has been shown between Si-HPMC associated with 1×10^6 hNC and Si-HPMC/XLG associated with 5×10^6 hNC. These results are in agreement with the literature as Janer et al. showed the internalization of nanoclays inside the cells [34]. Indeed, nanoclays induced apoptosis and were found in cytoplasmic vesicles of exposed cells. In the meantime, several groups have been working on the development of clay-based hydrogels and showed that cells remain viable in either 2D and 3D [20,35,37].

Altogether, our results demonstrate that when XLG are prepared as a suspension, they can be internalized and show some toxicity from 10 μg/L. However, when they are formulated as a gel, XLG increased the mechanical properties of the final construct while cells appear to remain viable in 2D and 3D (in the gelified form). The initial decrease of the cell density observed with Si-HPMC/XLG composite hydrogels could be overcome by decreasing the gel point or by increasing (5-fold) the number of cells used. This study validated the IPN hybrid hydrogel for cartilage tissue engineering in a nude mouse animal model. The larger animal model will then be used for the biocompatibility investigations of the products.

5. Conclusion

In conclusion, it has been demonstrated that adding XLG within Si-HPMC hydrogels increases the mechanical properties without interfering with the O_2 diffusion and cell viability after gelification. Therefore, the development of faster gelling composite hydrogel has to be evaluated. This could lead to an increase in the cell survival and the number of clusters. Their self-assembling capacity induces the formation of a hybrid interpenetrated network that enhances the stiffness of the hydrogel. The use of Si-HPMC/XLG hydrogels combined with chondrocytes in subcutis of nude mice has shown their potential use for cartilage tissue engineering. Investigation in the large animal model will have to be performed too thoroughly evaluate the preservation of the material inside a cartilage defect as well as the clinical relevance of our strategy.

Acknowledgements

We would like to thank, Pr. O. Malard (ENT surgery department, university hospital of Nantes, France), for providing human nasal cartilage and Dr F. Lejeune (Brétéché clinic, Nantes, France) for providing lipoaspirates. This research was supported by the regional program BIOREGOS (Pays de la Loire, France), by the Agence Nationale de la Recherche in the framework ANR-11-BSV5-0022 (HYCAR) and by FUI Marbiotech. LF was the recipient of a Nanofar Erasmus Mundus Doctorate fellowship.

References

[1] E.A. Makris, A.H. Gomoll, K.N. Malizos, J.C. Hu, K.A. Athanasiou, Repair and tissue engineering techniques for articular cartilage, Nat. Rev. Rheumatol. 11 (1) (2015) 21–34.
[2] C. Vinatier, C. Merceron, J. Guicheux, Osteoarthritis: from pathogenic mechanisms and recent clinical developments to novel prospective therapeutic options, Drug Discov. Today 21 (12) (2016) 1932–1937.
[3] J. Ringe, G.R. Burmester, M. Sittinger, Regenerative medicine in rheumatic disease-progress in tissue engineering, Nat. Rev. Rheumatol. 8 (8) (2012) 493–498.
[4] A.K. Gaharwar, C.P. Rivera, C.J. Wu, G. Schmidt, Transparent, elastomeric and tough hydrogels from poly(ethylene glycol) and silicate nanoparticles, Acta Biomater. 7 (12) (2011) 4139–4148.
[5] C. Merceron, C. Vinatier, J. Clouet, S. Colliec-Jouault, P. Weiss, J. Guicheux, Adipose-derived mesenchymal stem cells and biomaterials for cartilage tissue engineering, Joint Bone Spine 75 (6) (2008) 672–674.
[6] C. Merceron, S. Portron, M. Masson, B.H. Fellah, O. Gauthier, J. Lesoeur, Y. Cherel, P. Weiss, J. Guicheux, C. Vinatier, Cartilage tissue engineering: from hydrogel to mesenchymal stem cells, Biomed. Mater. Eng. 20 (3) (2010) 159–166.
[7] C. Vinatier, O. Gauthier, A. Fatimi, C. Merceron, M. Masson, A. Moreau, F. Moreau, B. Fellah, P. Weiss, J. Guicheux, An injectable cellulose-based hydrogel for the transfer of autologous nasal chondrocytes in articular cartilage defects, Biotechnol. Bioeng. 102 (4) (2009) 1259–1267.
[8] A.S. Hoffman, Hydrogels for biomedical applications, Adv. Drug Deliv. Rev. 54 (1) (2002) 3–12.
[9] K.Y. Lee, D.J. Mooney, Hydrogels for tissue engineering, Chem. Rev. 101 (7) (2001) 1869–1880.
[10] J.L. West, J.A. Hubbell, Photopolymerized hydrogel materials for drug delivery applications, React. Polym. 25 (2–3) (1995) 139–147.
[11] I. Levental, P.C. Georges, P.A. Janmey, Soft biological materials and their impact on cell function, Soft Matter 3 (3) (2007) 299–306.
[12] J.L. Drury, D.J. Mooney, Hydrogels for tissue engineering: scaffold design variables and applications, Biomaterials 24 (24) (2003) 4337–4351.
[13] J. Kopecek, Hydrogel biomaterials: a smart future?, Biomaterials 28 (34) (2007) 5185–5192
[14] F. Song, L.M. Zhang, J.F. Shi, N.N. Li, Viscoelastic and fractal characteristics of a supramolecular hydrogel hybridized with clay nanoparticles, Colloids Surf. BBiointerfaces 81 (2) (2010) 486–491.
[15] S.K. Agrawal, N. Sanabria-Delong, G.N. Tew, S.R. Bhatia, Nanoparticle-reinforced associative network hydrogels, Langmuir 24 (22) (2008) 13148–13154.
[16] K. Haraguchi, H.-J. Li, Mechanical properties and structure of polymer–clay nanocomposite gels with high clay content, Macromolecules 39 (5) (2006) 1898–1905.
[17] L.-M. Zhang, Y.-J. Zhou, Y. Wang, Novel hydrogel composite for the removal of water-soluble cationic dye, J. Chem. Technol. Biotechnol. 81 (5) (2006) 799–804.
[18] G. Schmidt, A.I. Nakatani, P.D. Butler, A. Karim, C.C. Han, Shear orientation of viscoelastic polymer–clay solutions probed by flow birefringence and SANS, Macromolecules 33 (20) (2000) 7219–7222.
[19] G. Schmidt, A.I. Nakatani, C.C. Han, Rheology and flow-birefringence from viscoelastic polymer-clay solutions, Rheologica Acta 41 (1–2) (2002) 45–54.
[20] J.I. Dawson, J.M. Kanczler, X.B. Yang, G.S. Attard, R.O. Oreffo, Clay gels for the delivery of regenerative microenvironments, Adv. Mater. 23 (29) (2011) 3304–3308.
[21] L.Z. Zhao, C.H. Zhou, J. Wang, D.S. Tong, W.H. Yu, H. Wang, Recent advances in clay mineral-containing nanocomposite hydrogels, Soft Matter 11 (48) (2015) 9229–9246.
[22] X. Bourges, P. Weiss, A. Coudreuse, G. Daculsi, G. Legeay, General properties of silated hydroxyethylcellulose for potential biomedical applications, Biopolymers 63 (4) (2002) 232–238.
[23] X. Bourges, P. Weiss, G. Daculsi, G. Legeay, Synthesis and general properties of silated-hydroxypropyl methylcellulose in prospect of biomedical use, Adv. Colloid Interface Sci. 99 (3) (2002) 215–228.
[24] S. Portron, C. Merceron, O. Gauthier, J. Lesoeur, S. Sourice, M. Masson, B.H. Fellah, O. Geffroy, E. Lallemand, P. Weiss, J. Guicheux, C. Vinatier, Effects of in vitro low oxygen tension preconditioning of adipose stromal cells on their in vivo chondrogenic potential: application in cartilage tissue repair, PLoS One 8 (4) (2013) e62368.
[25] C. Vinatier, D. Magne, A. Moreau, O. Gauthier, O. Malard, C. Vignes-Colombeix, G. Daculsi, P. Weiss, J. Guicheux, Engineering cartilage with human nasal chondrocytes and a silanized hydroxypropyl methylcellulose hydrogel, J. Biomed. Mater. Res. A 80 (1) (2007) 66–74.
[26] C. Merceron, S. Portron, M. Masson, J. Lesoeur, B.H. Fellah, O. Gauthier, O. Geffroy, P. Weiss, J. Guicheux, C. Vinatier, The effect of two- and three-dimensional cell culture on the chondrogenic potential of human adipose-derived mesenchymal stem cells after subcutaneous transplantation with an injectable hydrogel, Cell Transplant. 20 (10) (2011) 1575–1588.
[27] U. Tritschler, I. Zlotnikov, P. Fratzl, H. Schlaad, S. Gruner, H. Colfen, Gas barrier properties of bio-inspired Laponite-LC polymer hybrid films, Bioinspir. Biomim. 11 (3) (2016) 035005.
[28] J. Yoo, S.B. Lee, C.K. Lee, S.W. Hwang, C. Kim, T. Fujigaya, N. Nakashima, J.K. Shim, Graphene oxide and laponite composite films with high oxygen-barrier properties, Nanoscale 6 (18) (2014) 10824–10830.
[29] X. Bourges, M. Schmitt, Y. Amouriq, G. Daculsi, G. Legeay, P. Weiss, Interaction between hydroxypropyl methylcellulose and biphasic calcium phosphate after steam sterilisation: capillary gas chromatography studies, J. Biomater. Sci. Polym. Ed. 12 (6) (2001) 573–579.
[30] N. Buchtova, G. Rethore, C. Boyer, J. Guicheux, F. Rambaud, K. Valle, P. Belleville, C. Sanchez, O. Chauvet, P. Weiss, J. Le Bideau, Nanocomposite hydrogels for cartilage tissue engineering: mesoporous silica nanofibers interlinked with siloxane derived polysaccharide, J. Mater. Sci. – Mater. Med. 24 (8) (2013) 1875–1884.
[31] O. Bas, E.M. De-Juan-Pardo, C. Meinert, D. D'Angella, J.G. Baldwin, L.J. Bray, R.M. Wellard, S. Kollmannsberger, E. Rank, C. Werner, T.J. Klein, I. Catelas, D.W.

Hutmacher, Biofabricated soft network composites for cartilage tissue engineering, Biofabrication 9 (2) (2017) 025014.
[32] R.M. Domingues, M. Silva, P. Gershovich, S. Betta, P. Babo, S.G. Caridade, J.F. Mano, A. Motta, R.L. Reis, M.E. Gomes, Development of injectable hyaluronic acid/cellulose nanocrystals bionanocomposite hydrogels for tissue engineering applications, Bioconjugate Chem. 26 (8) (2015) 1571–1581.
[33] F.A. Formica, E. Ozturk, S.C. Hess, W.J. Stark, K. Maniura-Weber, M. Rottmar, M. Zenobi-Wong, A Bioinspired Ultraporous Nanofiber-Hydrogel Mimic of the Cartilage Extracellular Matrix, Adv. Healthcare Mater. 5 (24) (2016) 3129–3138.
[34] G. Janer, E. Fernandez-Rosas, E. Mas del Molino, D. Gonzalez-Galvez, G. Vilar, C. Lopez-Iglesias, V. Ermini, S. Vazquez-Campos, In vitro toxicity of functionalised nanoclays is mainly driven by the presence of organic modifiers, Nanotoxicology 8 (3) (2014) 279–294.
[35] K. Haraguchi, T. Takehisa, M. Ebato, Control of cell cultivation and cell sheet detachment on the surface of polymer/clay nanocomposite hydrogels, Biomacromolecules 7 (11) (2006) 3267–3275.
[36] M. Barandun, L.D. Iselin, F. Santini, M. Pansini, C. Scotti, D. Baumhoer, O. Bieri, U. Studler, D. Wirz, M. Haug, M. Jakob, D.J. Schaefer, I. Martin, A. Barbero, Generation and characterization of osteochondral grafts with human nasal chondrocytes, J. Orthop. Res. 33 (8) (2015) 1111–1119.
[37] B.P. Nair, M. Sindhu, P.D. Nair, Polycaprolactone-laponite composite scaffold releasing strontium ranelate for bone tissue engineering applications, Colloids Surf. B Biointerfaces 143 (2016) 423–430.